LIMNOLOGY and OCEANOGRAPHY

ASLO

Limnol. Oceanogr. 9999, 2020, 1–13

doi: 10.1002/lno.11637

Temperature acclimation alters phytoplankton growth and production rates

Jacob Susanne Strock ,* **S. Menden-Deuer**
Graduate School of Oceanography, University of Rhode Island, Narragansett, Rhode Island

Abstract

Temperature is a major driver of phytoplankton growth and physiology, but despite decades of study on temperature effects, the influence of temperature fluctuations on the growth acclimation of marine phytoplankton is largely unknown. To address this knowledge gap, we subjected a coastal phytoplankton species, *Heterosigma akashiwo*, to ecologically relevant temperature shifts of 2–3°C, cumulatively totaling 3–16°C across a range from 6°C to 31°C over a 3-week period. Using a symmetric design, we show time dependent differences between growth rates and that these changes were related to the magnitude of the temperature shift, but not the direction. Cell size scaled inversely with temperature at a rate of −1.9 to −3.3%°C^{-1} at all except the highest temperature treatments > 25°C. Intraspecific variability in growth rates increased exponentially with cumulative thermal shifts, suggesting thermal variability may be a driver of intraspecific variation. The observed acclimation effects on phytoplankton growth rates suggest that ignoring acclimation effects could systematically under or overestimate temperature-dependent primary production. Empirical results, contextualized with in situ coastal ocean temperature record, demonstrated that daily primary production could differ from current model assumptions utilizing acclimated rates by −33% to +36%. If broadly applicable to diverse phytoplankton species, these results have ramifications for predicting the ecology and production of phytoplankton in present day dynamic ecosystems and in future climate scenarios where thermal variability is expected to increase.

Through sheer magnitude of abundance, phytoplankton are responsible for primary production in the range of 49–60 Gt C yr^{-1} globally (Carr et al. 2006). Thus, phytoplankton characteristics like size, species composition, and physiology are fundamental to understanding everything from global nutrient cycling (Moore et al. 2013), carbon sequestration and export (Siegel et al. 2016), fisheries production (Kiørboe 1993), eutrophication (Hecky and Kilham 1988), and harmful algal blooms (Smayda 1997). The role of phytoplankton in these processes has led to decades of research seeking to quantify universal predictors for phytoplankton production and growth, such as temperature (Eppley 1972), light (Ryther 1956), and nutrients (Redfield 1958).

Temperature is a fundamental driver of physiological processes and critically important for predicting growth and production rates and yet, current models of phytoplankton physiology hinge on biological rates obtained under thermally static conditions. Thermal reaction norms (i.e., thermal performance curves) are the standard to quantify the response of phytoplankton growth to temperature (Boyd et al. 2013; Baker et al. 2016; Bestion et al. 2018), and can serve to explain performance and species prevalence patterns (Anderson and Rynearson 2020). Standard procedure dictates that thermal reaction norms are calculated using growth rates from organisms which are acclimated to a target temperature treatment. By these standards, acclimation is defined as a steady response and may take 1–3 weeks to achieve (Brand and Guillard 1981; Montagnes and Franklin 2001). Such controlled procedures impose assumptions of thermal stability, and well-adjusted physiology on the resulting data, including population scale growth. These assumptions of acclimation and stability are then propagated to other scales, such as to the community. Static conditions have been used to describe community scale production (Eppley 1972), and from there ecosystem and even global production (Antoine et al. 1996). More recent carbon-based production models have forgone the connections to temperature norms and instead use observationally derived relationships with temperature (Behrenfeld et al. 2005). These observational relationships average thermal conditions over space and time so the discrete effects of thermal variability on production are not resolved. Models using assumptions of achieved thermal acclimation and stability that predict the ecological function of phytoplankton may potentially lose accuracy especially in some of the most productive places in the ocean, like the coast (Cloern et al. 2014) and upwelling zones (Eppley et al. 1979) which are characteristically thermally dynamic.

*Correspondence: jstrock@uri.edu

Thermal acclimation in organismal physiology and growth are common and have been described for organisms ranging from lizards, to land-plants, and soil microbes (Tsuji 1988; Schimel et al. 2007; Ow et al. 2008), but have been undescribed for marine phytoplankton. Although unknown, it is likely that thermal variation alters phytoplankton physiology and thus, we expect phytoplankton growth rates and production in marine ecosystems to differ from the acclimated state. Despite decades of experiments involving temperature manipulation and marine phytoplankton growth, acclimation to thermal treatment has generally gone unreported, and therefore, there is little expectation for the nature or shape of the growth acclimation response. Considering population growth rate is a high-level characteristic that encompasses a multitude of interacting physiological and molecular underpinnings, growth in a fluctuating environment could reasonably be higher or lower than the acclimated response. In a freshwater green alga, directionality of thermal shifts mattered for the observable difference between acclimated and unacclimated growth rates (Kremer et al. 2018). The most closely related studies on thermal acclimation in marine phytoplankton, performed on three diatom taxa, focused on the photosynthetic pathway, enzymatic activity, and transcription (William and Morris 1982; Anning et al. 2001; Liang et al. 2019). These studies reported acclimation of short-term processes, such as enzyme abundance, pigment concentration, and photosynthetic production, finding that unacclimated responses were vastly different from the acclimated response (William and Morris 1982; Anning et al. 2001). Transcriptional response of species of the marine diatom genus *Chaetoceros* have shown both up- and downregulation of metabolic pathways from cell constituents (amino acids, lipids) to cell growth and death as cells acclimated to different temperatures (Liang et al. 2019). The preceding studies of thermal acclimation describe the unacclimated response across the thermal niche width, where changes in temperature were as great as 30°C (William and Morris 1982; Anning et al. 2001; Kremer et al. 2018). Such extreme temperature shifts are unlikely to occur even in shallow coastal ecosystems due to the high heat capacity of water. Thus, there exists a critical gap in knowledge of how small to moderate changes in temperature (< 5°C), which are most prevalent in the ocean, may impact population growth and primary production in marine systems.

Here we investigate if and how, realistic warming and cooling affects the growth rate and size of phytoplankton. As a model organism, we chose a common phytoplankter from the coastal environment, an ecosystem where high production (Smith and Mackenzie 1987), and high variability in environmental conditions, including in temperature are coincident; *Heterosigma akashiwo* is cosmopolitan (Honjo 1992) and capable of high biomass monospecific blooms (Li and Smayda 2000). This species' competitive ability across a broad range of temperature and salinity (Tomas 1978), as well as the tendency to form toxic blooms (Khan et al. 1997), make it an interesting subject individually, but also as a representative for phytoplankton ecology more generally. Considering *H. akashiwo* is thermally robust one may not expect sensitivity to temperature fluctuations. Thus, if a meaningful acclimation response were observed in this species, it would be an important indicator for future acclimation studies in other, likely more temperature sensitive species and recommend inclusion of acclimation effects into predictive models that incorporate primary production. Through laboratory experiments, we first measured the difference between unacclimated and acclimated growth rates and then evaluated the ramifications of incorporating the acclimation response into modeled primary production for different coastal habitats.

Methods

Experimental setup

Heterosigma akashiwo (CCMP 3374) was isolated from Narragansett Bay 10 June 2010 when in situ water temperature was 21.2°C. Since isolation, the culture was maintained at 15°C. Experiments were conducted with cells that were grown in autoclaved, 0.2 μm sterile-filtered seawater (30–31 ppt) amended with F/2 media without silica (Guillard 1975). Cultures were maintained at a light intensity of 150 μmol photons m^{-2} s^{-1} and a 12 : 12 h light : dark cycle. Preliminary experiments to determine the growth characteristics of this strain were used to maintain cultures in exponential phase by transferring cultures as needed every 4–10 d (depending on growth temperature), resulting in cell densities of 500–24,000 cell mL^{-1}. To avoid convolution of the thermal response with the response to new media, cultures were only transferred to new media more than 1 d prior to and 1 d post to a change in temperature (Grabski and Tukaj 2008).

Temperature treatments

With little prior information as to which features of changing temperature might influence growth, two major traits were examined in the experimental design: (1) the direction of temperature change (increasing or decreasing) and (2) the magnitude of temperature change (small shifts vs. larger cumulative changes). To address these features, and represent realistic rates of change, cultures were shifted sequentially to new growth temperatures outward from 15°C (Fig. 1). Including the control culture, growth rate, and acclimation was measured at 10 temperatures: 6°C, 8°C, 10°C, 12°C, 15°C, 18°C, 22°C, 25°C, 28°C, and 31°C. As each incubator had a static temperature, we used small discrete shifts in temperature over time. Beginning with the culture that was acclimated to 15°C, every 4 d a triplicate set of the cultures growing at the highest and lowest current temperatures were split, with one fraction retained at its current temperature and the other fraction shifted one temperature step outward (i.e., further toward the temperature extremes of 6°C and 31°C; Fig. 1). After

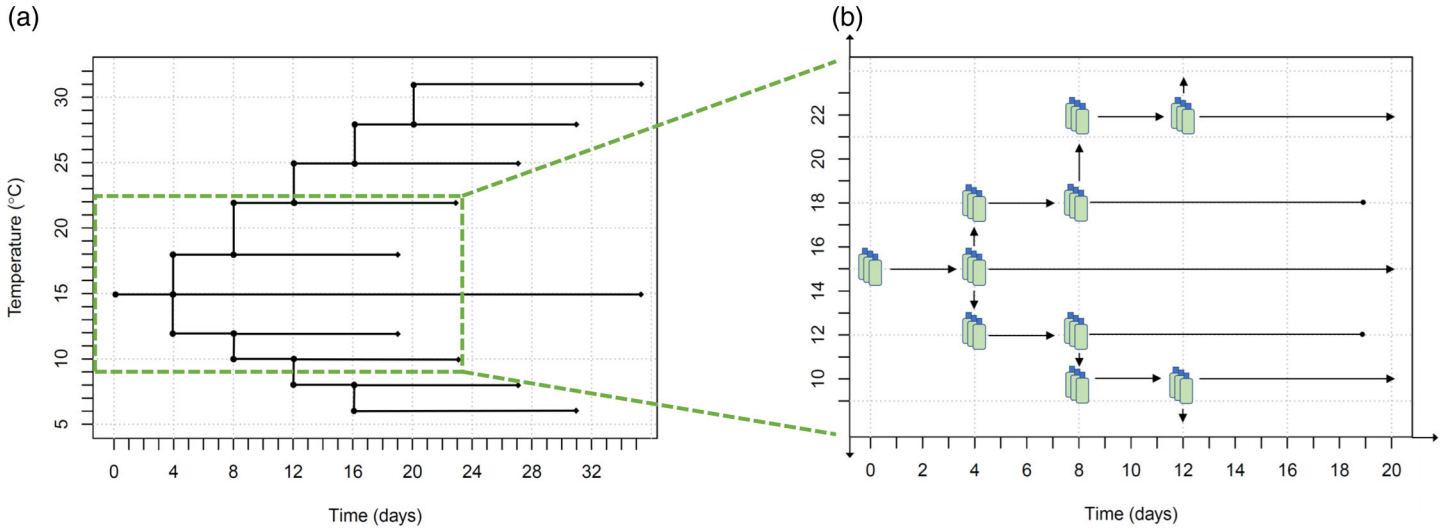

Fig. 1. Quantifying effects of directionality and magnitude of temperature shifts on phytoplankton growth rate. Left (**a**) symmetric experimental design across the entire temperature gradient. Black horizontal lines denote the period of observation. Vertical lines represent splitting of the culture, and transfer of triplicates to a new temperature treatment. Right (**b**) detail of the first two temperature shifts, where triplicate cultures illustrations mark a splitting event, arrows denote the direction of the temperature change, and horizontal lines cover the period of observation.

placement in a particular temperature treatment, cultures were maintained in exponential growth phase. Cultures maintained at 15°C throughout the duration of the experiment served as an acclimated control, and acted as a reference for the temporal consistency in acclimated rates. Through this design, cultures which had been subjected to a greater number of shifts saw a greater cumulative magnitude in temperature change. The magnitudes of temperature change for both increases and decreases in temperature were comparable. It took 16 d to complete the individual temperature shifts at 4-d intervals to reach both the coldest and warmest temperature treatments. Cell abundance and cell size were recorded daily for each culture at each treatment temperature for 15 d.

Dedicated incubators were used to regulate the temperature for cultures in the control (15°C, Model 2015 Low Temperature Incubator, VWR Scientific); 4°C, 6°C (I-41LLVL, Percival Scientific); 8°C, 18°C, 22°C (I-36LLVL, Percival Scientific); and 10°C treatments (Environ Air, Holman Engineering). The treatments of 25°C, 28°C, and 31°C were performed in clear 10-liter baths controlled by a coupled aquarium heater and thermostat (Fluval, Tru Temp), housed in an illuminated incubator. Light intensity was consistently controlled across temperature treatments.

Population and growth rate measurements

To quantify changes in cell size, population growth rate (specific growth rate), and volumetric growth rate, the abundance and cell size (equivalent spherical diameter [ESD]) distribution of each culture were measured with a 100 μm aperture on a Beckman Coulter Multisizer 3 (Beckman Coulter, Brea California 2020). The default bin size was the instrument standard of 0.2 μm. Each treatment set was measured daily for 15 d following the initial transfer to the target temperature. Experiments were terminated after 15 d because the objective of these experiments was to establish the response to relatively short-term temperature fluctuations. We recognize that longer periods of static conditions could have shown a continued acclimation process, although weeks of stable conditions are not likely to be ecologically meaningful in coastal environments.

Statistical analysis

Mean and standard deviation (SD) of cell size distribution and cell abundance, as measured by the Coulter Counter, were estimated from the raw data by a Gaussian distribution, fit with maximum likelihood estimation to the size of particles greater than 8 μm. This method avoided user selection bias (Menden-Deuer et al. 2020) and allowed rapid processing of 450 acquired files. Measurements that immediately followed culture inoculation and those from the stationary phase of growth were omitted. Cell volumes were estimated using ESD and spherical shape approximation. Cell biomass was calculated using ESD measured with the Coulter Counter and calculated cell volume with the relationship of $\text{pg C cell}^{-1} = 0.288 \times \text{volume}^{0.811}$ (Menden-Deuer and Lessard 2000). Total biomass was approximated as the product of the ESD and cell abundance.

Specific growth rate was calculated by linear regression of natural log-transformed abundance. Production rates were calculated by linear regression of natural log-transformed total biomass for each culture. Hereafter we use the term growth rate to refer implicitly to both specific growth and production rates which did not significantly differ from a 1 : 1 proportionality (*see* "Results" section). Specific growth rates were used to fit a thermal reaction norm modified from Norberg (2004),

where a, b, and z are shape parameters, w the thermal niche width, T a given temperature, and $k(T)$ the specific growth rate at that temperature.

$$k(T) = a * e^{bT}\left[1 - \left(\frac{T - z}{w/2}\right)^2\right]$$

To quantify the effect of time (acclimation) on specific growth rate, the final rates (μ_f, $7 \le \Delta$ time ≤ 15 d) were subtracted from the initial rates, measured over the first 3 d (μ_0; Δ time ≤ 3 d) for each temperature treatment. To understand patterns in the variability of growth rate among replicates as a function of the cumulative temperature change ($|\Delta$Temperature$|$) and time (translated into a binary variable; t_0 and t_f to 0 and 1, respectively), an exponential relationship was fit to the SD of the specific growth rate (σ), where c, d, and e are regression coefficients.

$$\sigma = c * e^{d*|\Delta\text{Temperature}| - e*\text{time}}$$

Alternative model fits to the data were compared by Akaike information criterion (AIC). All statistical analyses were performed in R. ANOVA methods were performed from the "base" package. Post hoc comparisons of acclimation relative to the control were made by Dunnett's tests from the "DescTools" package (Signorell 2019). Comparisons of continuous response variables (i.e., growth rates, ESD) were made by model II regression from the "lmodel2" package (Legendre 2018).

Acclimation ramifications for primary production simulations

To better understand how changes in temperature can alter ecosystem production, we conducted simulations using temperature record from three coastal buoys with distinct thermal histories that are within the thermal niche of *H. akashiwo*. Temperature data (1 h resolution from 2018) were obtained from the NOAA National Centers for Environmental Information. Water temperature at these stations, Honolulu, HI (21°18.4′N, 157°52′W, NOAA 1612340), Newport, RI (41°30.2′N, 71°19.6′W, NOAA 8452660) and St. Petersburg, Tampa Bay, FL (27°45.6′N, 82°37.6′W, NOAA 8726520), are driven by different phenomena. For example, the temperate site in RI is seasonally forced by atmospheric changes while the temperature in FL is strongly influenced by advection and mixing of water masses. These sites also differ at short scale (daily) variability, with the mean daily temperature ranges of 0.5°C, 1.3°C, and 1.1°C for HI, RI, and FL, respectively. The data from these sites for the complete year were used to quantify the potential discrepancy between unacclimated production vs. the assumption of perfectly acclimated production. Further, under the assumption that the environment selects for phytoplankton growing close to their thermal maxima, additional model scenarios were restricted to cases where the average temperature during the thermal history window was within 5°C of the thermal optimum at 21°C (17°C, 26°C), representing 40% of the total thermal niche window. This assumes the phytoplankton community is generally suited to the thermal environment.

Daily phytoplankton production was compared using acclimated and unacclimated growth rates inferred from our empirical measurements. The acclimated growth rate was interpolated from the empirically derived thermal performance curve that was constructed with the long-term specific growth rates from our experiments (7–15 d post-temperature change). The unacclimated growth rate applied a correction to this rate and was interpolated from the difference between the unacclimated and acclimated specific growth rates observed in the experiments which were dependent upon the magnitude of temperature change (*see* "Results" section). To calculate the unacclimated production for a given day, the simulation considered the range of water temperature of the previous 16 d. This time frame was chosen because in our experiment, the cumulative magnitude in temperature change over 16 d determined the difference between the unacclimated and acclimated growth rates. In the design of our experiment, 16 d were needed to expose cells to the full range of temperatures from 6°C to 31°C in modest steps of 2–4°C. Thus, in the model the in situ temperature range in a 16-d period informed how to modify growth rate to represent the unacclimated response. Consistent with the results where different magnitudes of temperature change elicited different acclimation responses, we applied a correction equal to the difference in initial and final growth rates observed at each magnitude in temperature change. Specifically, three temperature ranges in the thermal history window elicited different responses: 3–5°C, 5–13°C, or greater than 13°C (*see* "Results" section). The average specific growth rate difference (i.e., acclimation) for these three thermal ranges were -0.14 d^{-1}, 0.10 d^{-1}, and -0.18 d^{-1}, respectively. These differences were added to the acclimated rate interpolated from the thermal performance curve. That is, when the thermal history window had a temperature range of 3–5°C, 5–13°C, or greater than 13°C, a -0.14, 0.10, or -0.18 d^{-1} correction was added to the growth rate inferred from the thermal performance curve. Cases where no growth was observed were omitted. The percent difference between final and initial growth responses were compared for each day.

As an example, consider calculating the production for 1 d at the RI site. We first calculate the acclimated rate by plugging in the temperature to the Norberg equation of the thermal performance curve. Given a current temperature of 15°C, the thermal performance curve gives acclimated growth rate of 0.46 d^{-1} (from results). The unacclimated rates are inferred in a second step, by adding an acclimation factor. These acclimation factors were determined from the range in temperature during the 16-d thermal history. If over the previous 16 d, the maximum temperature was 19°C and minimum was 12°C, Δ temperature equals 7°C. From our experimental results, we then would adjust the acclimated growth rate up

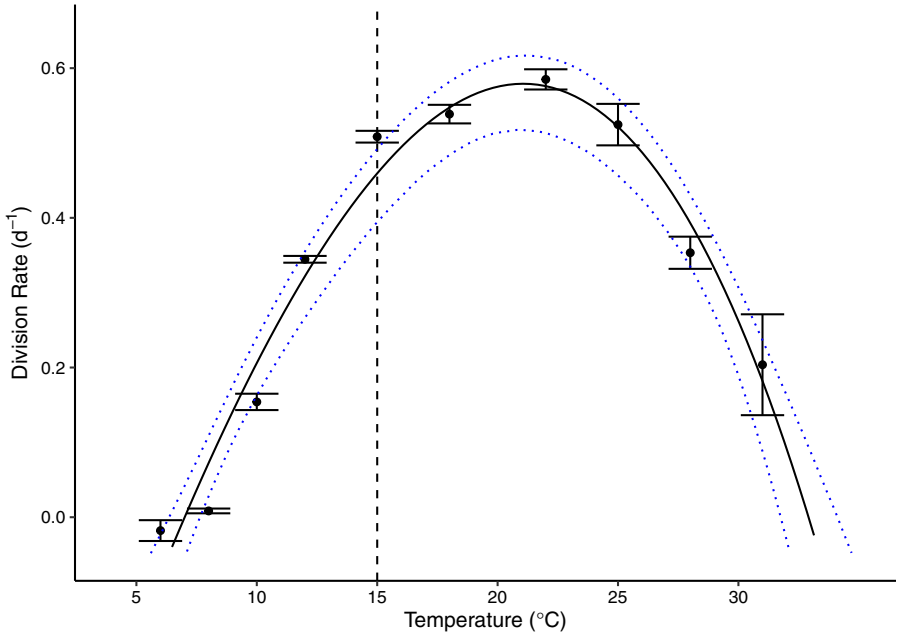

Fig. 2. Average ± SE of final growth rates (d^{-1}) at each temperature. The thermal reaction norm (Norberg 2004, eq. 1) calculated by maximum likelihood estimation with parameters a = 0.44°C, b = 0.013°C, z = 20.0°C, w = 25.9°C. The control temperature (15°C) is designated by the dashed vertical line. The bootstrapped 95% CI is shown by the dotted envelope. This fit suggests a thermal optimum (T_{opt}) of 21.0°C, and critical temperature minimum and maximum (CT_{min}, CT_{max}) of 7.0°C and 32.9°C.

0.10 d^{-1} to give an unacclimated growth rate of 0.56 d^{-1}. Therefore, the difference in daily production is the difference between using the 0.46 and 0.56 d^{-1} growth rate.

Results

Thermal reaction norm

Final growth rates (μ_f) obtained between 7 and 15 d after exposure to target temperature ranged from −0.02 ± 0.02 d^{-1} at 6°C to 0.58 ± 0.02 d^{-1} at 22°C (Fig. 2). The parameters of the Norberg thermal performance curve based on final specific growth rates for each temperature treatment indicate a maximum growth rate at 21.0°C, a thermal niche width (w) of 25.9°C, and shape parameters (a, b, and z) of 0.44°C, 0.013°C, and 20.0°C, respectively (Fig. 2). Inter- and extrapolation of this fit suggests a thermal optimum (T_{opt}) of 21.0°C, and a critical temperature minimum and maximum (CT_{min}, CT_{max}) of 7.0°C and 32.9°C, respectively.

Size changes

Cell size generally declined as temperature increased, except at the two highest temperature treatments (28°C and 31°C), where mean cell size increased with temperature (Fig. 3). Average cell size was largest (17.3 ± 0.97 μm) in the coldest treatment (6°C) and smallest at 25°C (10.3 ± 0.73 μm). A piecewise linear regression of size as a function of temperature yielded better coefficients of determination than a linear model across all temperatures. Separating cell size at temperature treatments up to 25°C from those above and including 28°C optimized AIC with a coefficient of determination (AIC = 1638, $p < 0.001$, $R^2 = 0.65$) as compared to a simple linear model of size across all temperatures (AIC = 1919, $p < 0.001$, $R^2 = 0.44$). There was a significant difference between the two slopes (two-sample z-test, $p < 0.001$). ESD declined with increasing temperature up to and including 25°C at −0.34 μm°C^{-1}. This represents a relative size reduction

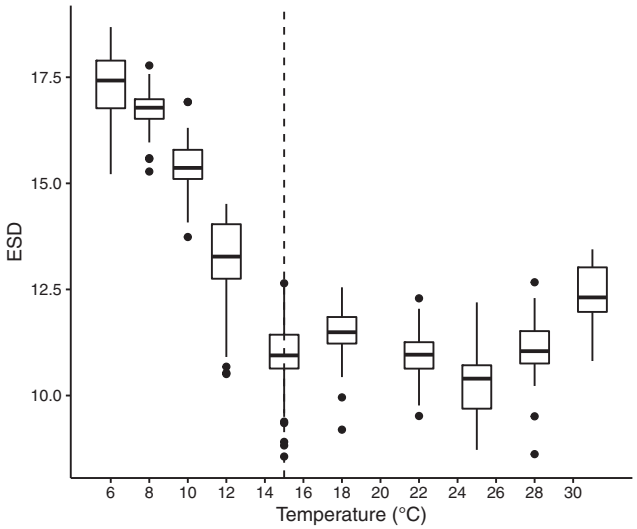

Fig. 3. Mean ESD (μm) for each temperature treatment using all cultures and time points (n = 45 per temperature). Each horizontal bar shows the median, box represents the 2nd and 3rd quartile, vertical lines extend to a multiple of 1.5 the interquartile range, and points are outliers.

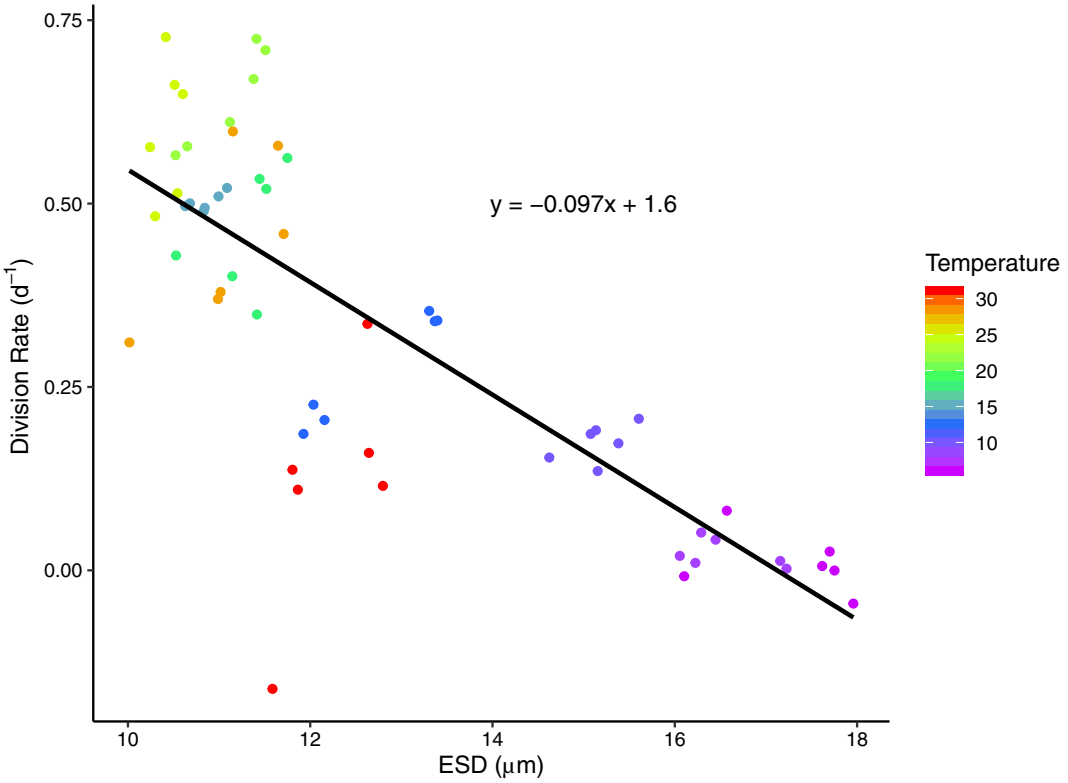

Fig. 4. Mean ESD (μm) and specific growth rate (division rate, d^{-1}) at each temperature treatment, denoted by color, with warmer colors indicating higher temperatures. Fit of model II regression resulted in an intercept of 1.6 d^{-1} and slope of −0.097 d^{-1} μm^{-1} ($p < 0.001$, $R^2 = 0.63$) and is shown with a black line.

of −1.9 to −3.3% °C^{-1}. Above 25 °C, cell size increased at a rate of 0.44 μm °C^{-1}.

Cell size was inversely related to specific growth rate. Average size decreased significantly with increasing specific growth rate, as shown by model II regression, predicting a proportionality of -0.097 ± 0.015 d^{-1} μm^{-1} ($p < 0.001$, $R^2 = 0.63$; Fig. 4). However, the specific growth rate at the highest temperature treatment (31°C) deviated most from this relationship. At this temperature, near CT_{max}, size features were poorly predicted by both temperature and specific growth rate. These data, however, were not influential points in the regression; exclusion affected the slope 6% and within the margin of error. The regression reported here includes all temperature treatments.

Temperature and time dependent growth: Acclimation

Cultures remained in exponential growth following changes in temperature. This indicates that irrespective of the fact that a temperature shift occurred and irrespective of the absolute temperature, exponential growth rates could be maintained. However, the growth rates did change over the 15-d observation period. Responses were classified by the difference (Δ) between the immediate, unacclimated, growth rate (< day 3) and the final growth rate (between days 7 and 15). Differences (Δ) in specific growth rate differed depending on the magnitude of the temperature change but not as a function of direction (Fig. 5). Three distinct response groups were identified, small and large temperature changes induced negative Δ specific growth rates with initial growth rates lower than final growth rates and intermediate temperature changes induced positive Δ specific growth rates, with initial growth rates higher than final growth rates (Fig. 5). The first response type was for the smallest magnitude of temperature change, control ± 3°C, Δ specific growth rates were negative (Dunnett's test, $p < 0.041$). The second response type coincided with intermediate to large total changes in temperature ($|\Delta T|$ = 5–13°C), which resulted in positive Δ specific growth rates (Dunnett's test, $p < 0.036$), that is, specific growth rate increased over time relative to the immediate rate. The third response type coincided with growth rates near the thermal maximum (ΔT = +16°C) which, similar to the smallest magnitude of temperature change had negative Δ specific growth rates (Dunnett's test, $p < 0.024$). The average Δ specific growth rates for these three groups were −0.14 d^{-1}, 0.10 d^{-1}, and −0.18 d^{-1}, respectively. The changes in growth rate over time were consistent within these three temperature treatment groups, regardless of the *direction* of temperature change.

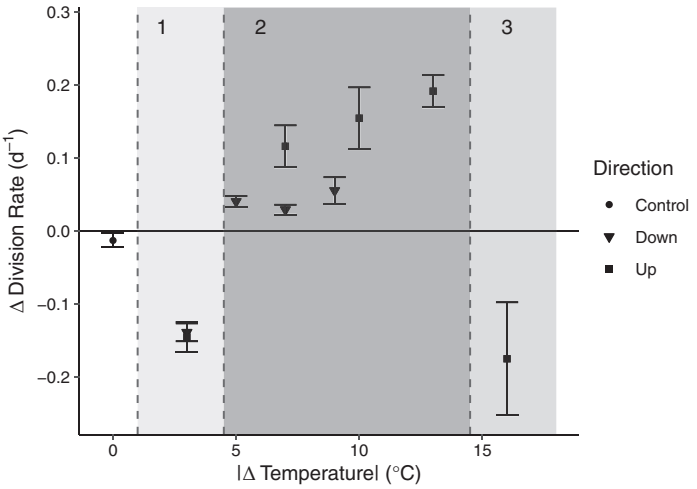

Fig. 5. Average ± SE difference in specific growth rate (Δ division rate, d^{-1}) between initial and final rates as a function of the magnitude of temperature change. The directionality of the temperature shift relative to the control is designated by shape (● = control, ▼ = down, ■ = up). Three response groups are designated by number and background shade: 1. Small magnitude temperature shifts result in initially lower growth; 2. Initially higher growth after intermediate to high temperature shifts; 3. Variable, and initially lower growth after extreme temperature shift near the thermal maximum. Directionality of the temperature shift did not affect the growth rate shift.

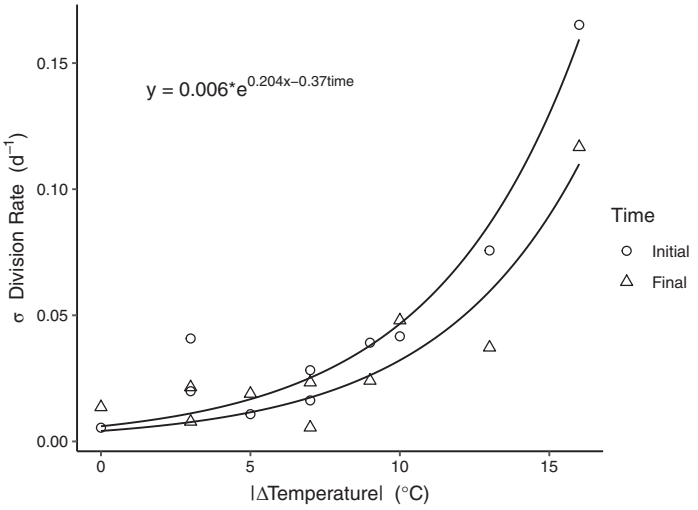

Fig. 6. Standard deviation of specific growth rate (division rate, d^{-1}) among cultures as a function of the absolute magnitude of temperature change, for initial (○) and final (△) growth rates. The fit shown is the nonlinear regression $\sigma_{\text{growth rate}} = 0.006*e^{0.204*\text{temperature}-0.37*\text{time}}$ ($p < 0.01$).

Growth metrics: Abundance and biomass based

Temperature-dependent changes in growth rate offset the proportionality of cell size and temperature, so that ultimately abundance and biomass-based growth rates were not significantly different from each other. A model II regression between both metrics showed that the 1 : 1 proportionality matched the regression slope of 1.00 and was within the 95% confidence interval (CI) of the slope [0.89, 1.13], $R^2 = 0.80$. Biomass-based growth followed a similar pattern as abundance-based changes. The exception were temperature shifts at the highest temperature where immediate growth rates were close to 0.

Temperature and time sensitive variance

Although cultures were clonally derived and sample size within each culture was large, replicates at each treatment showed considerable variability in specific growth rate that was proportional to both magnitude of temperature shifts and time. As shown by nonlinear regression, the SD of specific growth rates increased exponentially with the cumulative magnitude of temperature shift and decreased with time ($p < 0.01$, Fig. 6).

Production simulation

To quantify the potential impact of using unacclimated growth rates in predicting primary production, we calculated the difference in daily primary production for three coastal systems. By design, all sites showed distinct thermal histories, with the Honolulu, HI location representing equatorial and open ocean dynamics, Narragansett Bay, RI a temperate coastal estuary with strong seasonality and St. Petersburg, FL a subtropical bay with apparent influence of lower frequency events (Fig. 7). On a daily scale, the HI site had a median temperature range of 0.4°C and 99% of days with a range less than 1.0°C. In contrast, the RI site had a daily, median temperature range of 1.2°C, with 25% of days exceeding 1.6°C. The FL site had a daily, median temperature range of 1.0°C, with 25% of days exceeding 1.4°C. Over the thermal history period considered in this simulation (16 d), the median temperature range was 1.3°C, 4.0°C, and 4.0°C, for the HI, RI, and FL sites, respectively (Fig. 7).

Across the three sites, the consequence of considering the unacclimated growth response varied greatly. At the HI site, there was no 16-d window where the difference between the maximum and minimum temperature was greater than 3°C. At the RI site, 72% of the moving 16-d temperature-windows had temperature changes in excess of 3°C with 30% of days capturing temperature changes in the range of 5–13°C. At the FL site, 83% of the moving 16-d temperature-windows had temperature changes in excess of 3°C with 23% of days capturing temperature changes in the range of 5–13°C. At the HI site, because temperature fluctuated so little, unacclimated and acclimated growth rates were equal, and thus there was no difference in the calculated daily production. At the RI site, fluctuating temperatures lead to differences between unacclimated and acclimated growth rates and thus differences in the calculated daily production. Throughout the year, across all temperatures, the difference in daily production between estimates using unacclimated growth rates vs. acclimated growth rate

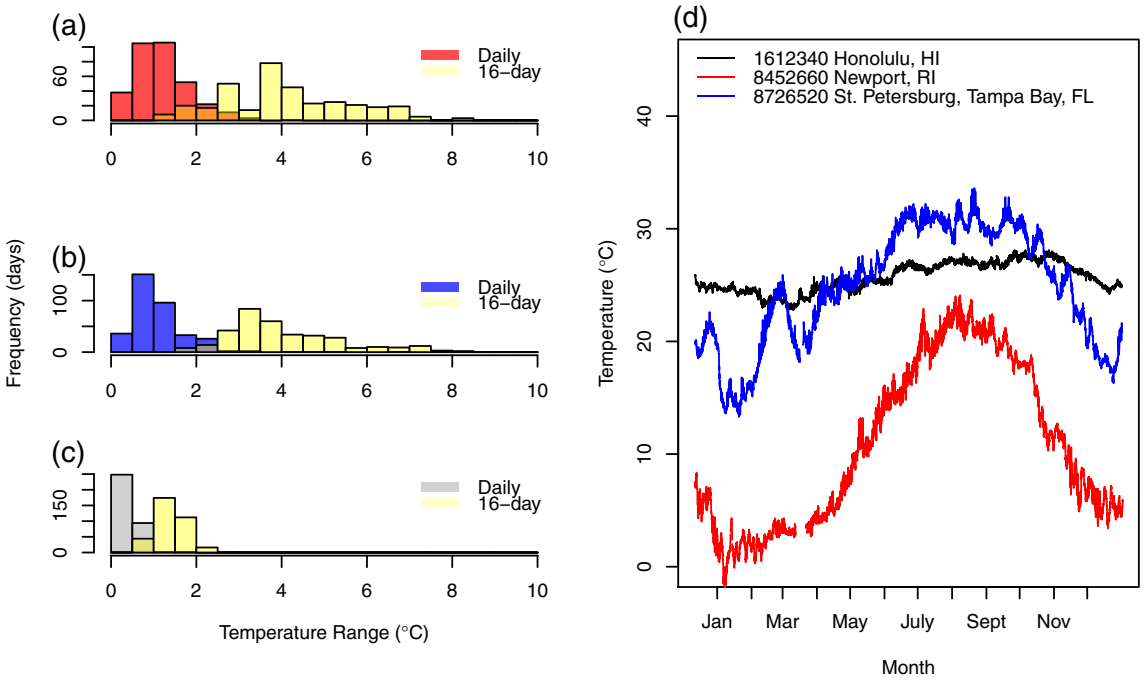

Fig. 7. Annual temperature history of three coastal sites of the NOAA National Centers for environmental information from stations 1612340 Honolulu, HI (21°18.4′N, 157°52′W); 8452660 in Newport, RI (41°30.2′N, 71°19.6′W); 8726520 St. Petersburg, Tampa Bay, FL (27°45.6′N, 82°37.6′W) collected at a resolution of 1 h^{-1} in 2018. Panels (**a**), (**b**), and (**c**) are the frequency distribution of 1-d and 16-d temperature range over 1 yr at Newport, St. Petersburg, and Honolulu sites, respectively. Panel (**d**) shows the full history of temperature at each site.

was −270% to 100% with a mean daily difference of −9% ± 51%. For cases at the RI site where average temperature was within 5°C of the thermal optimum, production ranged −30% to 36% with a mean 15% ± 23%. At the FL site, differences in production ranged from −75% to 97% of the unacclimated production, with a mean of 18% ± 42%. For cases at the FL site where average temperature was within 5°C of the thermal optimum, production ranged −33% to 33% with a mean −0.86% ± 28%. Aggregating both sites and comparing the acclimated and unacclimated production in each case, there was a small but highly variable average difference between the models (7% ± 27%). The differences in unacclimated vs acclimated production ranged from −270% to +100% from the acclimated model, and −33% to 36% under conditions within 5°C of the mean, expected to be most representative of community scale responses (Fig. 8).

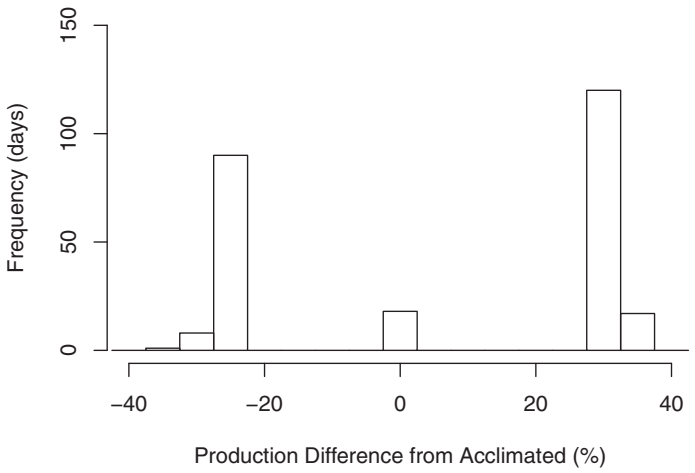

Fig. 8. Frequency of percent differences between model simulations of primary production assuming purely acclimated rates and an alternate model where growth rates were adjusted to reflect preacclimation rates for the temperature regime of the RI and FL coastal sites over the simulation period.

Discussion

To date, the role of temperature on the growth rate of phytoplankton has largely focused on quantifying physiological responses of fully acclimated cultures (Eppley 1972; Bissinger et al. 2008; Boyd et al. 2013; Wang et al. 2018). However, some of the most productive places in the ocean, like coastal regions, are also thermally highly variable environments. Whether cell physiology and ultimately growth rate, respond instantaneously to a changed temperature regime or carry lag effects from prior thermal regimes could significantly alter population growth and production rates. Such acclimation induced discrepancies in population growth rates have implications for estimating primary production and derived processes, such as export and trophic transfer.

Our temperature shift experiments demonstrate a measurable time-dependent growth response (acclimation) that remarkably was dependent on the magnitude but not the directionality of temperature change (i.e., warming or cooling). These findings show a clear need to recognize acclimation as a factor in quantifying marine primary production. This is a task not just valuable for interpreting currently variable and productive systems, but also one which may provide insight into future global climate where thermal variability is predicted to increase (Schär et al. 2004).

Growth rates showed consistent, time-dependent change as a function of the magnitude of the temperature shift regardless of directionality. The growth rate response across all cultures and treatments fell into three distinct groups, with growth rate increases observed over time for small (± 3°C) and extreme (+ 16°C) temperature shifts and decreases in growth rate in response intermediate temperature shifts (± 5–13°C). To our knowledge, these observations are not predicted by theory. Experiments which have used oscillating temperature treatments have generally shown lower growth rates in variable conditions (Bernhardt et al. 2018; Hutchins et al. 2019; Kling et al. 2020). In the closest example of a growth acclimation study, the freshwater green alga *Chlamydomonas reinhardtii* showed initial growth rates that were higher or lower than acclimated rates, depending if the culture had first come from an extreme high (33°C) or low (14°C) temperature treatment (Kremer et al. 2018). In that case, the directionality of temperature change was important in predicting acclimation. In contrast, under a symmetric treatment design and small increment thermal shifts as used here, the difference between unacclimated and acclimated rates were similar, irrespective of the directionality (i.e., warming or cooling). This finding is important because if the direction of temperature change is nonpredictive and reflective of natural systems, then modeling phytoplankton dynamics with a consideration for an acclimation process can be simplified.

Although in this study the direction of temperature change did not predict the acclimation response, the magnitude of thermal change was important. This too is distinct from the limited prior information. Indirect evidence of acclimation from a broad based meta-analysis of the Q_{10} of metabolic enzymes of marine ectotherms has suggested acclimated thermal rates are consistently lower than the unacclimated response to temperature change (Seebacher et al. 2015). In the context of the Q_{10} index and the data shown here, acclimated rates have a Q_{10} of 1.2, but if unacclimated rates were considered, this could either be lower, as was for 3°C shifts (Q_{10} = 1.0), or higher, as was for ≥ 5°C shifts (Q_{10} = 1.6). Our growth data show that the Q_{10} estimate and thermal response more generally rely on the magnitude of temperature change. Predictability of the growth rate from the magnitude of thermal change suggests using acclimated rates may lead to systematic bias in overestimating growth under small and cumulatively extreme (< 5°C, > 13°C) temperature change, and underestimating growth in intermediate to high (5°C < ΔT ≤ 13°C) temperature change.

The magnitude of temperature change was an important predictor for whether the acclimation response was beneficial (growth increasing with time) or detrimental (decreasing with time). While the physiological and molecular mechanisms underlying the differentiation of growth rate changes into three groups would require a targeted analysis such as by transcriptomics, ecological theory regarding evolution and plastic responses suggests that it is not unexpected to observe a pattern where small changes could produce beneficial acclimation while larger changes induce detrimental responses. This magnitude-dependent response holds some consistency with theory which suggests that in highly variable environments, the cost of thermal-mismatch can exceed the potential benefit of acclimation, and thereby, physiological responses may be most representative of some average environmental state (Fischer et al. 2011). In the context of this experiment, the design is representative of a scenario where the environment continues to change so that the costs of adaptive plasticity to a specific temperature may outweigh the benefits. Thereby, organisms subjected to successive environmental changes may be developing a more general acclimation strategy. Another explanation, also suggested by Kremer et al. 2018, was that detrimental acclimation could be representative of bet hedging. Bet hedging could be represented whereby cells invest in cellular components such as heat shock proteins for high temperatures (Schuster et al. 1988) or ribosomal proteins to overcome translational inefficiency at low temperatures (Toseland et al. 2013). These are examples of molecular responses that could represent bet hedging for more extreme conditions, increasing energetic cost, and thus resulting in apparently detrimental acclimation responses.

Near the thermal limits, response of cell size, specific growth rate, and acclimation differed from responses across the thermal niche. This difference indicates that at temperatures near the thermal limits, temperature dependence is governed by different metabolic trade-offs. At high temperature treatments, cell size increased with temperature contrary to the decrease across other treatments, and at maximum, the 31°C treatment, the proportionality of size and specific growth rates was far below the linear relationship characteristic of cooler treatments. This difference in proportionality could mean that at high temperature, heat stress reduces investment in division and other maintenance, and cellular demands take precedence. Such a difference in metabolism would be consistent with the expected stresses at high temperatures, which may affect photosystem II, membrane structure, and trigger pathways such as those for heat-shock proteins (Schuster et al. 1988). Such stress responses could explain size, division, production, and acclimation observations at high temperature that deviated from the consistent relationships across all other treatments. These results also suggest poor predictability of high temperature responses based on the remainder of the thermal response.

At any treatment level, despite temperature-related differentiation in cell size in general, there was no discernable difference between specific growth and production rates or between change in specific growth and change in production rates. Cell size—at all but the two highest temperatures above the thermal optima—showed a decrease of −1.9 to −3.3%° C^{-1}, which is consistent with the prediction of Atkinson et al. (2003) for all protists. These changes in cell size have the potential to make biomass production a more or less sensitive metric to temperature change. However, here, variation in specific growth rates dominated over cell size variation and thereby proportionality between specific growth and biomass-based growth was maintained. For this reason, we report specific growth rates, which by our methods are more exact and not encumbered by multiplicative uncertainties in both size and abundance. The consistency observed here between specific growth and production differed from what has been observed in marine microzooplankton (Franzè and Menden-Deuer 2020) with the implication that different trophic levels may be disproportionately affected by thermal disturbance. Nevertheless, despite the consistency between specific growth and production seen in this study, the acclimation effects on growth rate shown here suggest caution for modeling phytoplankton productivity in thermally dynamic environments, which in cases like coastal zones, can be highly productive (Cloern et al. 2014) and thus rapidly translate to considerable discrepancies between predictions and observations at larger scales.

The in situ temperature-dependent simulation of production demonstrated the potential for major discrepancy between the unacclimated and acclimated response. In our analysis, there were large differences between predictions based on acclimated vs. unacclimated growth rates. Overall, on the annual scale, model differences were not statistically distinguishable from zero because under- and overestimates were balanced. However, discrete deviations of the unacclimated model ranged as much as between 270% lower to 100% higher than production estimated by purely acclimated rates. Within 5°C of the temperature optimum, deviations from −33% to 36% might be a more accurate representation of community scale response in natural systems. While communities may be characterized by broader performance functions (Kling et al. 2020), if these deviations are applicable to diverse plankton communities, it would suggest acclimation and scale are critical. For temporal and spatial scales of days and meters, acclimation could greatly matter as evidenced by the considerable deviations in production estimates shown here. Differences in production vastly exceed measurement uncertainty and highlight the potential for serious discrepancy between acclimated rates derived in static laboratory conditions, and realized rates in dynamic natural systems. Models which integrate over large space and time scales may on average be accurate but likely miss discrete processes in a dynamic system. Given the nonlinear nature of biological processes, for example, consumer-resource relationships, the underlying dynamics of plankton population dynamics and their ramifications for large scale processes may be missed.

The model outcomes comparing production estimates based on different acclimation assumptions also suggests that thermal variability could partially contribute to interannual variability in phytoplankton bloom formation (Li and Smayda 2000) and explain the difficulty to predict bloom timing (Smayda 1998). These observations may also shed light on why production for phytoplankton aggregated within layers was measured to be higher than for plankton within the rest of the water column, because these layers provide a presumably more static environment (Menden-Deuer 2012). However, environmental variability and plankton patchiness are not considered a predictor of bloom dynamics, despite theoretical and empirical evidence that static and variable environments impose selective pressures for different ecological strategies (Barton et al. 2010) including phenotypic plasticity (Miner et al. 2005). Our experimental observations of acclimation to temperature change, which are further elucidated by model simulations show that phytoplankton production can be enhanced or depressed depending on the magnitude of temperature change. For this reason, quantifying the numerical response under variable conditions—as shown here—may be vital for predicting population and community dynamics.

Here, we also saw a diversifying effect of temporal heterogeneity in environmental conditions, whereby variation in growth increased with the frequency and magnitude of temperature shifts. Previously, functional diversity at the population level had been attributed to spatial heterogeneity by triggering plastic response (Bucci et al. 2012). However, theory and model simulations show that spatial heterogeneity is insufficient to maintain intra-specific variability (Menden-Deuer and Rowlett 2014). This is further evidenced by experiments with clonal replicates under identical environmental conditions, which frequently show intra-specific variability (Boyd et al. 2013; Harvey et al. 2015). Our results suggest that temporal thermal variability in itself may be a driver of physiological variation through acclimation. Such physiological variation can affect population productivity, stability, and contribute to the maintenance of genetic diversity (Bolnick et al. 2011). Thus, temperature fluctuations onto themselves could be a driver of plankton diversity, an effect that can be exacerbated as environmental variability is anticipated to increase.

The responses presented here are derived from the raphidophyte *H. akashiwo*, while the acclimation response likely differs by taxa, functional type, and thermal scenario. Even at the inter-strain level, the functional traits of *H. akashiwo* have been shown to significantly differ (Harvey et al. 2015), posing a challenge to plankton ecologists in general. While we do not mean to imply that the responses observed here are universally applicable across phylogenetic groups, we do believe the results provide the insight that

acclimation has substantial ramifications for the prediction of oceanic primary production and needs to be accounted for. Notably, there are infinite other thermal histories that could be also meaningfully utilized in an experimental design to test different starting temperatures, rates of change, alternating directions of change, and patterns (e.g., oscillatory temperature exposure). In this experiment, each acute temperature exposure was associated with a specific trajectory of thermal history (i.e., changes were made in steps of 2–4°C). To achieve and observe the modest temperature shift treatments in this study, in triplicate, for 15 d, 450 experimental observations were required. It is quite likely that other fluctuations, like subdiel oscillation in a shallow coastal fjord would yield different acclimation responses. Despite the opportunity for greater phylogenetic representation and alternate experimental designs, this experiment clearly shows that unacclimated phytoplankton production differs from the assumption of instantaneous acclimation. Thus, this work sheds light on the need to emphasize the dynamic nature of coastal habitats and the ramifications of environmental variability for primary production.

Conclusion

For the growth acclimation response of phytoplankton, there are a limited number of possible response scenarios. The first has been the general assumption that temperature–time gradients have no effect on growth and thus ecosystem models. Although phytoplankton acclimation data were lacking, the scenario of instantaneous acclimation is in disagreement with observations for diverse organisms which have been studied with respect to their acclimation capacity (Tsuji 1988; Schimel et al. 2007; Ow et al. 2008). At the opposite end of the spectrum are scenarios where thermal change results in mortality. While situationally this may be true, time-series observations of plankton communities are evidence that temperature change is not always fatal (Karentz and Smayda 1984). In-between these response extrema, the results presented here evidence what may be more common: a gradual acclimation response that results in significant changes in primary production. Here, we demonstrate quantitatively that marine phytoplankton growth rates are sensitive to temperature change and that these physiological responses have ramification for derived ecosystem processes, including primary production.

References

Anderson, S. I., and T. A. Rynearson. 2020. Variability approaching the thermal limits can drive diatom community dynamics. Limnol. Oceanogr. **65**: 1961–1973. https://doi.org/10.1002/lno.11430

Anning, T., G. Harris, and R. Geider. 2001. Thermal acclimation in the marine diatom Chaetoceros Calcitrans (Bacillariophyceae). Eur. J. Phycol. **36**: 233–241. https://doi.org/10.1080/09670260110001735388

Antoine, D., J.-M. André, and A. Morel. 1996. Oceanic primary production: 2. Estimation at global scale from satellite (coastal zone color scanner) chlorophyll. Global Biogeochem. Cycles **10**: 57–69. https://doi.org/10.1029/95GB02832

Atkinson, D., B. J. Ciotti, and D. Montagnes. 2003. Protists decrease in size linearly with temperature: ca. 2.5% °C. https://doi.org/10.1098/rspb.2003.2538

Baker, K. G., C. M. Robinson, D. T. Radford, A. S. McInnes, C. Evenhuis, and M. A. Doblin. 2016. Thermal performance curves of functional traits aid understanding of thermally induced changes in diatom-mediated biogeochemical fluxes. Front. Mar. Sci. **3**: 44. https://doi.org/10.3389/fmars.2016.00044

Barton, A. D., S. Dutkiewicz, G. Flierl, J. Bragg, and M. J. Follows. 2010. Patterns of diversity in marine phytoplankton. Science **327**: 1509–1511. https://doi.org/10.1126/science.1184961

Behrenfeld, M. J., E. Boss, D. A. Siegel, and D. M. Shea. 2005. Carbon-based ocean productivity and phytoplankton physiology from space. Global Biogeochem. Cycles **19**: 1–14. https://doi.org/10.1029/2004GB002299

Bernhardt, J. R., J. M. Sunday, P. L. Thompson, and M. I. O'Connor. 2018. Nonlinear averaging of thermal experience predicts population growth rates in a thermally variable environment. Proc. R. Soc. B Biol. Sci. **285**: 20181076. https://doi.org/10.1029/2004GB002299

Bestion, E., C.-E. Schaum, and G. Yvon-Durocher. 2018. Nutrient limitation constrains thermal tolerance in freshwater phytoplankton. Limnol. Oceanogr.: Lett. **3**: 436–443. https://doi.org/10.1002/lol2.10096

Bissinger, J. E., D. J. S. Montagnes, J. Harples, and D. Atkinson. 2008. Predicting marine phytoplankton maximum growth rates from temperature: Improving on the Eppley curve using quantile regression. Limnol. Oceanogr. **53**: 487–493. https://doi.org/10.4319/lo.2008.53.2.0487

Bolnick, D. I., and others. 2011. Why intraspecific trait variation matters in community ecology. Trends Ecol. Evol. **26**: 183–192. https://doi.org/10.1016/J.TREE.2011.01.009

Boyd, P. W., and others. 2013. Marine phytoplankton temperature versus growth responses from polar to tropical waters – outcome of a scientific community-wide study. PLoS One **8**: e63091. https://doi.org/10.1371/journal.pone.0063091

Brand, L. E., R. R. L. Guillard and L. S. Murphy. 1981. A method for the rapid and precise determination of acclimated phytoplankton reproduction rates. J. Plankton Res. **3**: 193–201. https://doi.org/10.1029/GB001i003p00187

Bucci, V., D. Nunez-Milland, B. S. Twining, and F. L. Hellweger. 2012. Microscale patchiness leads to large and important intraspecific internal nutrient heterogeneity in phytoplankton. Aquat. Ecol. **46**: 101–118. https://doi.org/10.1007/s10452-011-9384-6

Carr, M. E., and others. 2006. A comparison of global estimates of marine primary production from ocean color. Deep-Sea Res. Part II Top. Stud. Oceanogr. **53**: 741–770. https://doi.org/10.1016/j.dsr2.2006.01.028

Cloern, J. E., S. Q. Foster, and A. E. Kleckner. 2014. Phytoplankton primary production in the world's estuarine-coastal ecosystems. Biogeosciences **11**: 2477–2501. https://doi.org/10.5194/bg-11-2477-2014

Eppley, R. 1972. Temperature and phytoplankton growth in the sea. Fish. Bull. **70**: 1063–1085.

Eppley, R. W., E. H. Renger, and W. G. Harrison. 1979. Nitrate and phytoplankton production in Southern California coastal waters. Limnol. Oceanogr. **24**: 483–494. https://doi.org/10.4319/lo.1979.24.3.0483

Fischer, B., B. Taborsky, and H. Kokko. 2011. How to balance the offspring quality–quantity tradeoff when environmental cues are unreliable. Oikos **120**: 258–270. https://doi.org/10.1111/j.1600-0706.2010.18642.x

Franzè, G., and S. Menden-Deuer. 2020. Common temperature-growth dependency and acclimation response in three herbivorous protists. Mar. Ecol. Prog. Ser. **634**: 1–13. https://doi.org/10.3354/meps13200

Grabski, K., and Z. Tukaj. 2008. Autoinduction activity of a conditioned medium obtained from high density cultures of the green alga *Scenedesmus subspicatus*. J. Appl. Phycol. **20**: 323–330. https://doi.org/10.1007/s10811-007-9260-x

Guillard, R. R. L. 1975. Culture of phytoplankton for feeding marine invertebrates, p. 29–60. *In* Culture of marine invertebrate animals. Springer. Boston, MA.

Harvey, E. L., S. Menden-Deuer, and T. A. Rynearson. 2015. Persistent intra-specific variation in genetic and behavioral traits in the Raphidophyte, *Heterosigma akashiwo*. Front. Microbiol. **6**: 1277. https://doi.org/10.3389/fmicb.2015.01277

Hecky, R. E., and P. Kilham. 1988. Nutrient limitation of phytoplankton in freshwater and marine environments: A review of recent evidence on the effects of enrichment. Limnol. Oceanogr. **33**: 796–822. https://doi.org/10.4319/lo.1988.33.4part2.0796

Honjo, T. 1992. Harmful red tides of Heterosigma akashiwo. NOAA Tech. Rep. **111**: 27–32. NMFS

Hutchins, D. A., P. Qu, F. X. Fu, J. Kling, M. Huh, and X. Wang. 2019. Distinct responses of the nitrogen-fixing marine cyanobacterium trichodesmium to a thermally-variable environment as a function of phosphorus availability. Front. Microbiol. **10**: 1282. https://doi.org/10.3389/fmicb.2019.01282

Karentz, D., and T. J. Smayda. 1984. Temperature and seasonal occurrence patterns of 30 dominant phytoplankton species in Narragansett Bay over a 22-year period (1959-1980). Mar. Ecol. Prog. Ser. **18**: 277–293. https://doi.org/10.3354/meps018277

Khan, S., O. Arakawa, and Y. Onoue. 1997. Neurotoxins in a toxic red tide of Heterosigma akashiwo (Raphidophyceae) in Kagoshima Bay, Japan. Aquac. Res. **28**: 9–14. https://doi.org/10.1046/j.1365-2109.1997.t01-1-00823.x

Kiørboe, T. 1993. Turbulence, phytoplankton cell size, and the structure of pelagic food webs. Adv. Mar. Biol. **29**: 1–72. https://doi.org/10.1016/S0065-2881(08)60129-7

Kling, J. D., M. D. Lee, F. Fu, M. D. Phan, X. Wang, P. Qu, and D. A. Hutchins. 2020. Transient exposure to novel high temperatures reshapes coastal phytoplankton communities. ISME J. **14**: 413–424.

Kremer, C. T., S. B. Fey, A. A. Arellano, and D. A. Vasseur. 2018. Gradual plasticity alters population dynamics in variable environments: Thermal acclimation in the green alga *Chlamydomonas reinhartdii*. Proc. R. Soc. B Biol. Sci. **285**: 20171942. https://doi.org/10.1098/rspb.2017.1942

Legendre, P. 2018. Lmodel2: Model II regression. R package. Available from https://cran.r-project.org/package=lmodel2

Li, Y., and T. J. Smayda. 2000. *Heterosigma akashiwo* (Raphidophyceae): On prediction of the week of bloom initiation and maximum during the initial pulse of its bimodal bloom cycle in Narragansett Bay. Plankton Biol. Ecol. **47**: 80–84.

Liang, Y., J. A. Koester, J. D. Liefer, I. Andrew, and Z. V. Finkel. 2019. Molecular mechanisms of temperature acclimation and adaptation in marine diatoms. ISME J. **13**: 2415–2425. https://doi.org/10.1038/s41396-019-0441-9

Menden-Deuer, S. 2012. Structure-dependent phytoplankton photosynthesis and production rates: Implications for the formation, maintenance, and decline of plankton patches. Mar. Ecol. Prog. Ser. **468**: 15–30. https://doi.org/10.3354/meps09968

Menden-Deuer, S., and E. J. Lessard. 2000. Carbon to volume relationships for dinoflagellates, diatoms, and other protist plankton. Limnol. Oceanogr. **45**: 569–579. https://doi.org/10.4319/lo.2000.45.3.0569

Menden-Deuer, S., and others. 2020. Multi-instrument assessment of phytoplankton abundance and cell sizes in mono-specific laboratory cultures and whole plankton community composition in the North Atlantic. Front. Mar. Sci. **7**: 254. https://doi.org/10.3389/fmars.2020.00254

Menden-Deuer, S. and J. Rowlett. 2014. Many ways to stay in the game: individual variability maintains high biodiversity in planktonic microorganisms. J. R. Soc. Interface **11**: https://doi.org/10.1098/rsif.2014.0031

Miner, B. G., S. E. Sultan, S. G. Morgan, D. K. Padilla, and R. A. Relyea. 2005. Ecological consequences of phenotypic plasticity. Trends Ecol. Evol. **20**: 685–692. https://doi.org/10.1016/J.TREE.2005.08.002

Montagnes, D. J., and M. Franklin. 2001. Effect of temperature on diatom volume, growth rate, and carbon and nitrogen content: reconsidering some paradigms. Limnology and oceanography, **46**: 2008–2018. https://doi.org/10.4319/lo.2001.46.8.2008

Moore, C. M., and others. 2013. Processes and patterns of oceanic nutrient limitation. Nat. Geosci. **6**: 701–710. https://doi.org/10.1038/ngeo1765

Norberg, J. 2004. Biodiversity and ecosystem functioning: A complex adaptive systems approach. Limnol. Oceanogr. **49**: 1269–1277. https://doi.org/10.4319/lo.2004.49.4_part_2.1269

Ow, L. F., D. Whitehead, A. S. Walcroft, and M. H. Turnbull. 2008. Thermal acclimation of respiration but not photosynthesis in *Pinus radiata*. Funct. Plant Biol. **35**: 448–461. https://doi.org/10.1071/FP08104

Redfield, A. 1958. The biological control of the chemical factors in the environment. Am. Sci. **46**: 230–205. https://www.jstor.org/stable/pdf/27827150

Ryther, J. H. 1956. Photosynthesis in the ocean as a function of light intensity. Limnol. Oceanogr. **1**: 61–70. https://doi.org/10.4319/lo.1956.1.1.0061

Schär, C., P. L. Vidale, D. Lüthi, C. Frei, C. Häberli, M. A. Liniger, and C. Appenzeller. 2004. The role of increasing temperature variability in European summer heatwaves. Nature **427**: 332–336. https://doi.org/10.1038/nature02300

Schimel, J., T. C. Balser, and M. Wallenstein. 2007. Microbial stress-response physiology and its implications for ecosystem function. Ecology **88**: 1386–1394. https://doi.org/10.1890/06-0219

Schuster, G., D. Even, K. Kloppstech, and I. Ohad. 1988. Evidence for protection by heat-shock proteins against photoinhibition during heat-shock. EMBO J. **7**: 1–6. https://doi.org/10.1002/j.1460-2075.1988.tb02776.x

Seebacher, F., C. R. White, and C. E. Franklin. 2015. Physiological plasticity increases resilience of ectothermic animals to climate change. Nat. Clim. Chang. **5**: 61–66. https://doi.org/10.1038/nclimate2457

Siegel, D. A., and others. 2016. Prediction of the export and fate of global ocean net primary production: The EXPORTS Science plan. Front. Mar. Sci. **3**: 22. https://doi.org/10.3389/fmars.2016.00022

Signorell, A. 2019. DescTools: Tools for descriptive statistics. R package. Available from https://cran.r-project.org/package=DescTools

Smayda, T. J. 1997. Harmful algal blooms: Their ecophysiology and general relevance to phytoplankton blooms in the sea. Limnol. Oceanogr. **42**: 1137–1153. https://doi.org/10.4319/lo.1997.42.5_part_2.1137

Smayda, T. J. 1998. Ecophysiology and bloom dynamics of *Heterosigma akashiwo* (Raphidophyceae). *In* D. M. Anderson, A. D. Cembella, and G. M. Hallegraeff 113–131. Physiological ecology of harmful algal blooms. Springer. Berlin.

Smith, S. V. and F. T. Mackenzie. 1987. The ocean as a net heterotrophic system: Implications From the carbon biogeochemical cycle. Global Biogeochem. Cycles **1**: 187–198. https://doi.org/10.1029/GB001i003p00187

Tomas, C. R. 1978. Olsthodiscus luteus (Chrysophycae) II. Formation and survival of a benthic stage. J. Phycol. **14**: 314–319. https://doi.org/10.1111/j.1529-8817.1978.tb00304.x

Toseland, A. et al. 2013. The impact of temperature on marine phytoplankton resource allocation and metabolism. Nat. Clim. Chang. **3**: 979–984. https://doi.org/10.1038/NCLIMATE1989

Tsuji, J. S. 1988. Thermal acclimation of metabolism in Sceloporus lizards from different latitudes. Physiol. Zool. **61**: 241–253. https://doi.org/10.1086/physzool.61.3.30161237

Wang, Q., Z. Lyu, S. Omar, S. Cornell, Z. Yang, and D. J. S. Montagnes. 2018. Predicting temperature impacts on aquatic productivity: Questioning the metabolic theory of ecology's 'canonical' activation energies. Limnol. Oceanogr. **64**: 1172–1185. https://doi.org/10.1002/lno.11105

William, K. W. L., and I. Morris. 1982. Temperature adaptation in *Phaeodactylum tricornutum* Bohlin: Photosynthetic rate compensation and capacity. J. Exp. Mar. Biol. Ecol. **58**: 135–150. https://doi.org/10.1016/0022-0981(82)90125-3

Acknowledgments

This material is based upon work supported in part by the National Science Foundation (EPSCoR Cooperative Agreement OIA-1655221, Biological Oceanography OCE-1736635) and the National Atmospheric and Space Administration campaigns (NAAMES NNX15AL2G, EXPORTS 80NSSC17K0716). Jacob Strock was supported by the National Space Grant College and Fellowship Program, Space Grant Opportunities (NASA STEM -NNX15AI06H). We appreciate logistical support from Amanda Montalbano, as well as help with experimental design and valuable feedback from Stephanie Anderson, Gayantonia Franzè, Victoria Fulfer, Heather McNair, and Tatiana Rynearson. We are thankful for the anonymous reviews which led to substantive improvement of this manuscript.

Conflict of Interest

None declared.

Submitted 10 October 2019
Revised 03 April 2020
Accepted 23 September 2020

Associate editor: K. David Hambright